# Berkovich nanoindentation study of 16 nm Cu/Nb ARB nanolaminate: Effect of anisotropy on the surface pileup

Rahul Sahay, Arief S Budiman, Christian Harito, Fergyanto Gunawan, Etienne Navarro, Stéphanie Escoubas, Thomas W Cornelius, Izzat Aziz, Pooi See Lee, Olivier Thomas, et al.

# Berkovich nanoindentation study of 16 nm Cu/Nb ARB nanolaminate: effect of anisotropy on the surface pileup

Rahul Sahay[1*], Arief S. Budiman[1,2*], Christian Harito[2], Fergyanto Gunawan[2], Etienne Navarro[3], Stéphanie Escoubas[3], Thomas W. Cornelius[3], Izzat Aziz[4], Pooi See Lee[4], Olivier Thomas[3] , Nagarajan Raghavan[1]

[1]Xtreme Materials Lab, Engineering Product Development, Singapore University of Technology and Design (SUTD), Singapore

[2]Industrial Engineering Department, BINUS Graduate Program – Master of Industrial Engineering, Bina Nusantara University, Jakarta, Indonesia

[3]Aix-Marseille Univ., Université de Toulon, CNRS, IM2NP, Marseille, France

[4]School of Materials Science and Engineering, Nanyang Technological University, Singapore

*Corresponding Authors: suriadi@alumni.stanford.edu, rahul@sutd.edu.sg

## Abstract

Nanoindentation is widely used to investigate elastic modulus, hardness, and work hardening behaviour of nano- and micro-scale laminates. In this work, 16 nm accumulative roll bonding (ARB) Cu/Nb nanolaminate is used as a test material due to its interfacial anisotropy owing to the presence of contrasting interfaces along rolling (RD) and transverse direction (TD). Nanoindentation was performed along TD as well as RD of ARB Cu/Nb nanolaminate and then Scanning Probe Microscopy (SPM) data was collected to measure the pile-up along RD and TD in the Cu/Nb nanolaminate. 16 nm Cu/Nb ARB nanolaminate along RD was found to show higher surface pile-up than TD which is attributed to crystallographic and interfacial anisotropy resulting in (a) higher yield strength (low plasticity) along TD in comparison to RD and (b) high interfacial sliding in the case of TD resulting in less co-deformation of layers in comparison to RD. This work highlights the significant importance of the surface pile-up phenomenon in facilitating the study of anisotropic behavior in micro/nano-laminates.

**keywords:** nanoindentation, nanolayers, pile-up, plastic deformation, hardness, laminates

## 1 Introduction

Nanoindentation is widely used to measure the local elastic/plastic, and time-dependent mechanical properties of thin films and small volumes of bulk materials. Nevertheless, the stress state generated by indentation is complex as compared to typical tensile/compression experiments. Therefore, the deformation during indentation usually is inhomogeneous as compared to tensile/compression experiments [1–3]. Further, it is highly likely (in the case of nanolaminate) that indent will form within a single grain resulting in a highly anisotropic deformation [4–7]. This anisotropic deformation can give rise to plastic deformation-induced residual impression during indentation such as pile-up or sink-in characteristic of the nanolaminate. In fact, this crystallographic anisotropy dependence on interface-mediated plasticity in nanolaminate has recently been observed and studied in detail using advanced microstructural/nanomechanical characterization techniques [8–12]. These pileups (residual impressions) can also help to identify the anisotropy characteristic of the nanolaminate.

The test material used in the present analysis is 16 nm Cu/Nb nanolaminates fabricated through accumulative roll bonding (ARB). Cu/Nb ARB nanolaminates have become the subject of experimental and theoretical studies due to their outstanding strength, thermal stability and radiation resistance [13–15]. These unique properties make it a promising new generation material for a wide range of applications, such as novel metallic flexible/stretchable conductor technology. This particular sample (16 nm Cu/Nb nanolaminates), for instance, has been shown to exhibit significantly larger extent of interfacial sliding (localized shear region either on the interfaces or very near the interfaces) [8–10] compared to similar Cu/Nb nanolaminate samples with larger individual layer thickness [16]. Furthermore, within the same individual layer thickness, interfacial sliding has been shown to be substantially larger

in TD compared to in RD [8–10, 16]. Such a strong anisotropy could manifest in the surface pile-up (or sink-in) in a nanoindentation experiment. Early investigations into the mechanical properties of Cu/Nb nanolaminates relied exclusively on nanoindentation results [17, 18]. In general, varieties of dislocation-based models for multilayer material systems have been developed to fit flow strength data derived from the indentation measurements. However, due to the inhomogeneous stress state associated with indentation measurements, a better understanding of the plasticity due to the anisotropy associated with Cu/Nb nanolaminates is required. To this end, nanoindentation is performed with the major axis aligned along TD as well as RD to study their surface pile-up and then associate them to the variation in the plasticity observed along TD as well as RD.

In this study, the mechanical behavior of 16 nm Cu/Nb ARB nanolaminates was investigated through nanoindentation experiments. Later, Oliver-Pharr method was employed to obtain the hardness and reduced Young's modulus of the Cu/Nb nanolaminates. In the present work, we performed nanoindentation to obtain load-displacement curves and surface pileup along both RD and TD as a function of the indentation depth. Also, the trend for surface pileup for both RD and TD is analyzed and then associated with the variation in the plasticity along these directions.

## 2 Materials and Methods

### 2.1 Material

Multilayer Cu/Nb (copper/niobium) nanolaminates were prepared by accumulative roll bonding (ARB) in collaboration with Dr. Irene Beyerlein and Dr. Nathan Mara (both formerly at the Los Alamos National Laboratory). ARB samples were synthesized by repeated rolling of 1 mm Nb sheet sandwiched between two 0.5 mm Cu sheets. These Cu/Nb stacks were repeatedly cut into half and re-stacked and then re-rolled to obtain polycrystalline multilayer

Cu/Nb nanolaminate [19]. The rolling direction was kept constant throughout the ARB process. Cu/Nb ARB samples used for the analysis have 16 nm nominal individual layer thicknesses. A 4-axis diffractometer (XPert, PanAlytical), shown in Figure 1 of the supplementary data, equipped with a Cu anode ($\lambda$ = 1.54184 A) and operated at 40 kV and 30 mA was used for pole figure measurements as presented in Figures 1 and 2 for copper and niobium, respectively. Here, angle psi was varied from 0° to 75° whereas phi was varied from 0° to 360° (here, phi = 0° corresponds to RD and phi = 90° corresponds to TD) to obtain diffraction patterns from predominant crystallographic planes for both copper and niobium. Cu/Nb (16 nm) ARB interfaces consist of a mixture of the {112} <111> Cu || {112} <110> Nb and {552} <110> Cu || {112} <110> Nb [20]. Further details of the ARB process and the texture evolution can be found in the literature [13, 20]. The grains in these nanolaminates become extremely elongated, with aspect ratios exceeding 1:50:5 (ND:RD:TD) at layer thicknesses ≤ 65 nm [21]. Further, plane strain deformation process of rolling generates anisotropy both in texture and grain morphology [22, 23]. Typically for Cu/Nb ARB samples, the stress required for the layers to shear along the RD is theoretically infinite as compared to 1.2 GPa for TD [24].

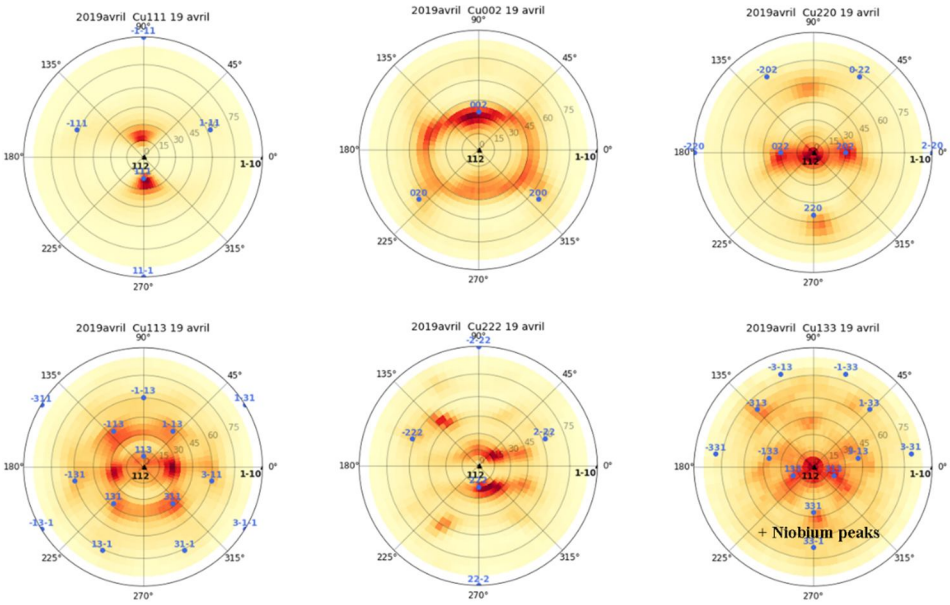

Figure 1. Pole Figure measurements of copper in Cu/Nb ARB nanolaminate using 4 axis diffractometer.

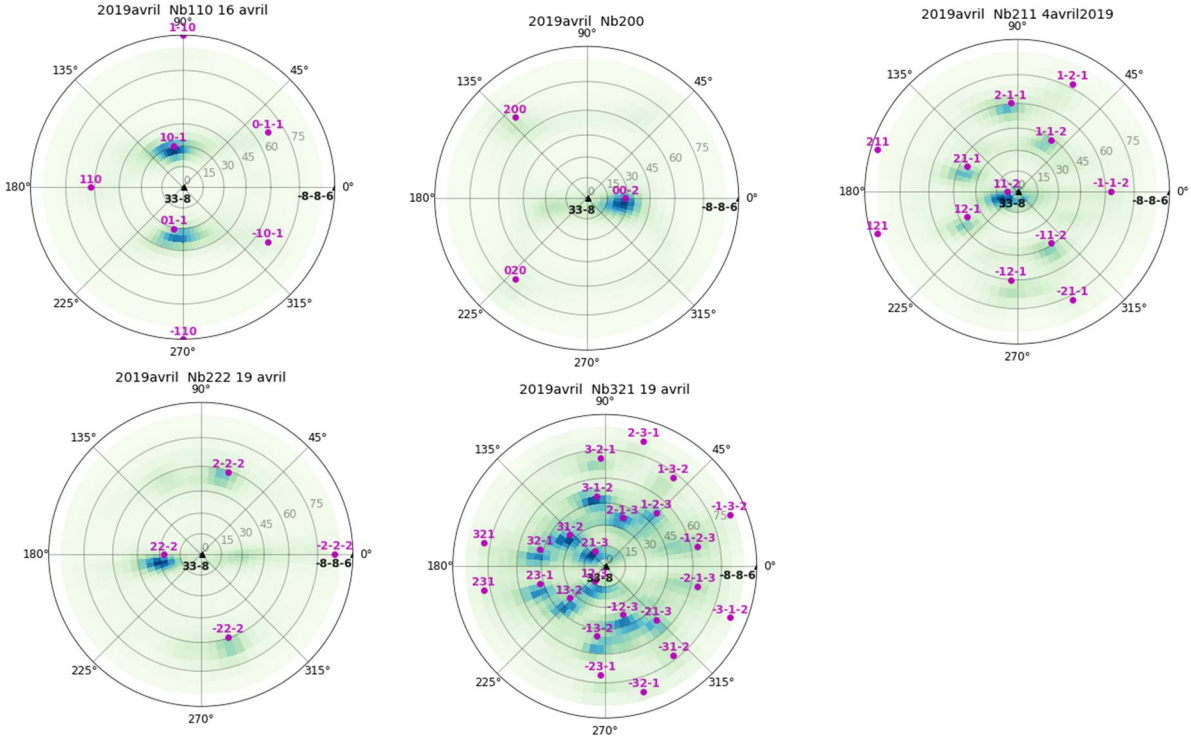


Figure 2. Pole Figure measurements of niobium in Cu/Nb ARB nanolaminate using 4 axis diffractometer.

## 2.2 Nanoindentation

Typically, during nanoindentation, a diamond indenter penetrates normally into a sample, and then the applied load (*P*) and displacement (*h*) are continuously recorded during the indentation cycle of loading and unloading. The load-displacement curve thus obtained is usually analyzed by the Oliver-Pharr method to obtain the mechanical properties of the samples. Nanoindentation experiments were performed using Hysitron Triboindenter TI 950 (make: Bruker Inc, USA) having displacement resolution ~0.2 nm and load resolution ~30 nN. The indentations were performed using a Berkovich tip in a continuous stiffness measurement mode. Prior to experiments, the Triboindenter is calibrated using a standard fused quartz sample for tip area function and machine compliance calibrations in order to precisely calculate contact stiffness using the Oliver-Pharr method. The tests were then performed in displacement control

mode with a loading displacement rate of 5 nm/s and an unloading displacement rate of 10 nm/s. The ratio of the specimen height to the maximum penetration depth is kept more than ~10 to avoid any substrate effect. The spacing between two indents was kept as ~20 μm to avoid any interaction between the plastic zone of indents.

### 2.3 Surface pileup profile

Scanning Probe Microscopy (SPM) included in Hysitron Triboindenter was used to map the profiles of the indents after nanoindentation. An area of 3 × 3 $\mu m^2$ including an indent was scanned to obtain profiles of the indents with high precision. Focused ion beam (FIB) milling (Zeiss Crossbeam 540) was used to polish the surface of the sample before indentation using low current of 1.5 nA at a voltage of 30 kV. The indented profiles were obtained on the polished sample surface to obtain height-profiles along RD and TD which were then used for measuring the pile-up along these directions.

## 3 Results and Discussion

### 3.1 Mechanical behaviour of 16 nm Cu/Nb ARB nanolaminate

Nanoindentation was used for the measurement of hardness, and reduced Young's modulus along RD and TD of 16 nm Cu/Nb ARB using Oliver-Pharr method [25]. Typically, in the case of Cu/Nb ARB nanolaminate, properties were found to vary with layer thickness. For instance, Beyerlein *et al.* [13] compared the hardness of Cu/Nb ARB nanolaminate as a function of layer thickness ranging from 714 nm to 7 nm. The hardness increased with the reduction in the layer thickness to an ultrahigh value of 5 GPa for layer thickness equal to 7 nm. This value is two orders of magnitude higher than those of Cu or Nb bulk materials.

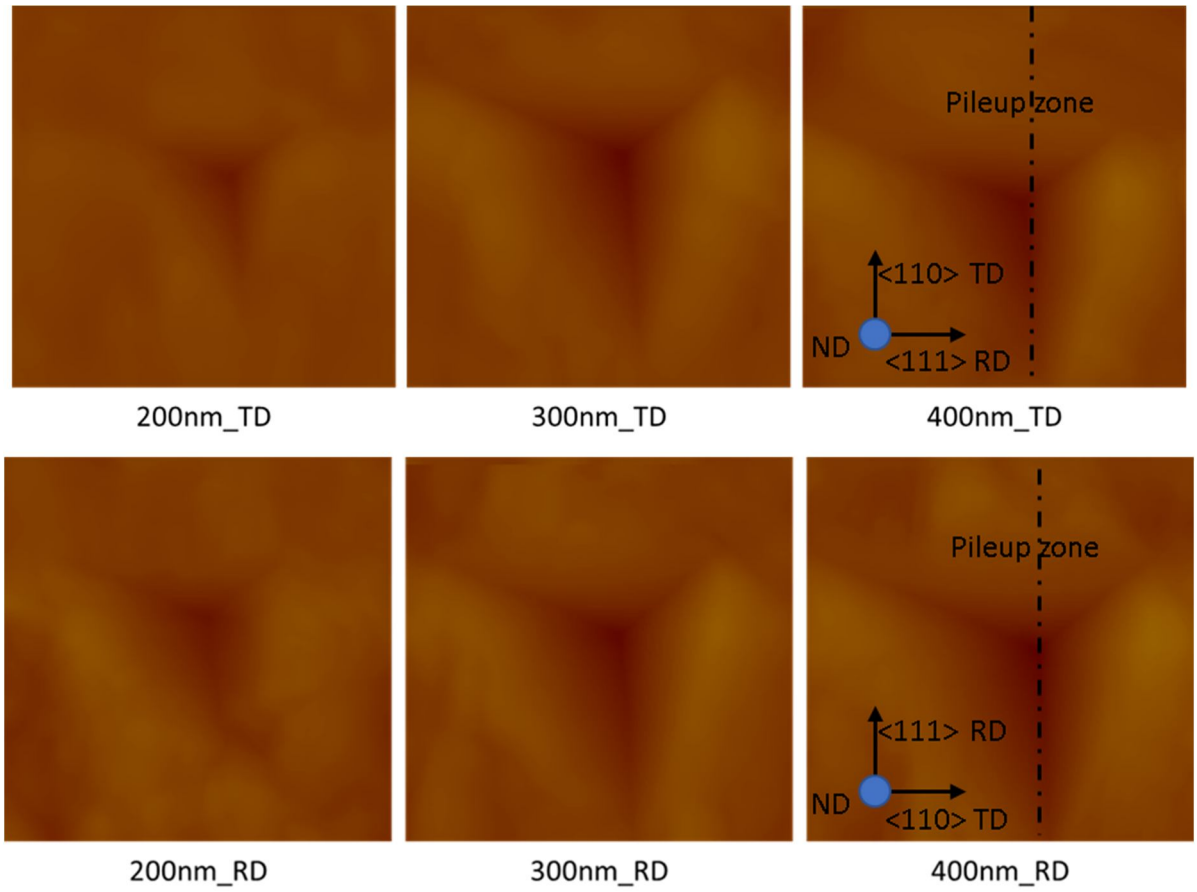


Figure 3. Figure shows Scanning Probe Microscopy (SPM) images of the indents for TD and RD as a function of indentation depth. The scanned area was 3 × 3 $\mu m^2$. These images are obtained after each indentation to accurately measure the height-profiles and corresponding pileups. Crystallographic directions are indicated for Niobium. The height profile is obtained along the major axis shown with a dotted line.

In this analysis, hardness and reduced Young's modulus of 16 nm Cu/Nb ARB nanolaminate were calculated as a function of indentation depth. Representative indents as a function of indentation depth are shown for TD and RD in Figure 3, and their corresponding load-displacement curves are shown in Figure 4. The experimentally obtained nanoindentation load-displacement curves depict an increase in the applied load with an increase in the indentation depth for both TD and RD. For both TD and RD, the indentation depth applied were 200 nm, 300 nm and 400 nm. Nevertheless, in the case of TD, the maximum indentation depth reached is 356.95 in comparison to applied 400 nm in the case of RD. The low achievable indentation

depth in the case of TD is attributed to its high yield in comparison to RD [26] which is also responsible for low pileup for TD in comparison to RD. Later, Oliver-Pharr method is used to calculate hardness and reduced Young's modulus from experimentally obtained load-displacement curves. The hardness of 16 nm Cu/Nb ARB was found to reduce from 4.33 GPa to 2.72 GPa and the Young's modulus reduced from 107.24 GPa to 92.72 GPa with an increase in the indention depth from 200 nm to 400 nm.

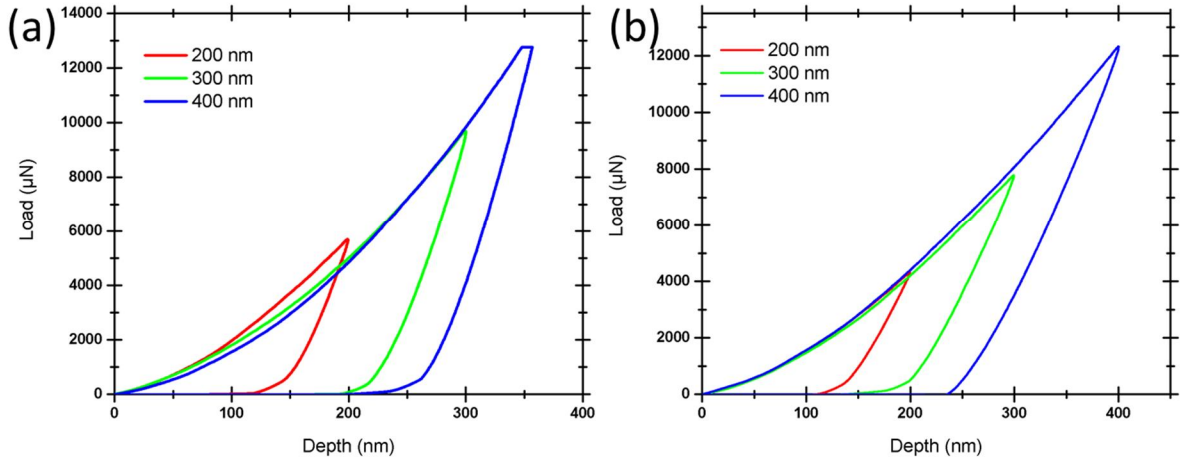


Figure 4. Figure shows the typical load-displacement curves obtained through nanoindentation for (a) TD and (b) RD as a function of indentation depth.

### 3.2 Pileup as a function of anisotropy of the 16 nm Cu/Nb ARB nanolaminate

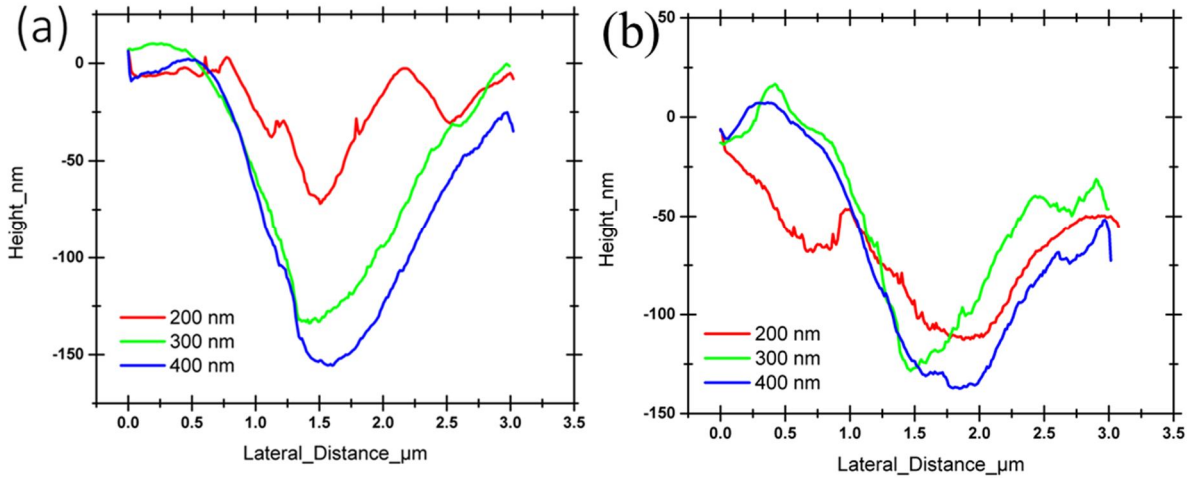


Figure 5. Height profiles along the major axis of indents used for measuring pileups along (a) TD and (b) RD as a function of the indentation depth.

The profiles of the indents were scanned using SPM. Height-profiles curves along the major axis of the indents were obtained which assisted in measuring the pileup along TD and RD. Figure 5 shows height-profile curves along TD and RD as a function of the indentation depth ranging from 200 nm to 400 nm. For the indentation depth less than 200 nm (such as 50 nm, 100 nm), pileups were small and, in some cases, comparable to the surface roughness and so were not easily distinguishable by SPM. As can be seen from Figure 6, the pile-up heights increase with an increase in the indentation depth for both RD and TD. Comparison of the pile-up heights along RD and TD show an increase in the pile-up height for RD in comparison to TD with an increase in the indention depth.

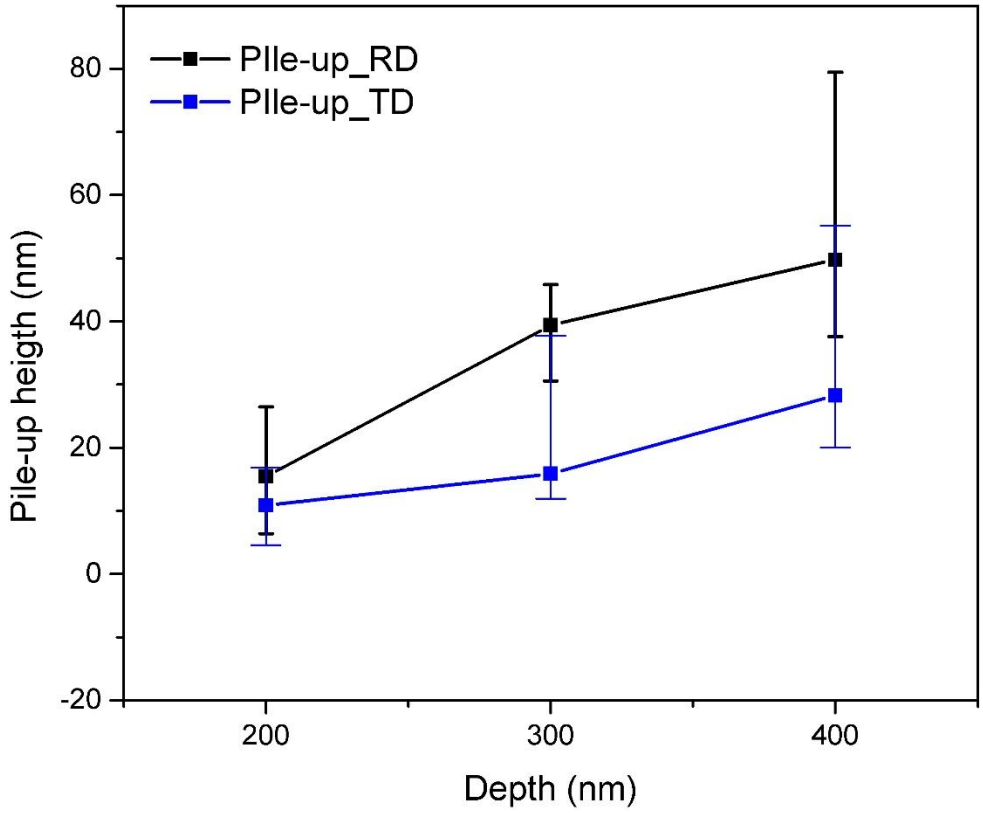


Figure 6. Comparison of the pile-up heights along RD and TD Cu/Nb nanolaminate as a function of the indention depth.

# 4 Discussion

## 4.1 Nanoindentation

During nanoindentation tests for nanolaminates, the dislocation nucleation, and their propagation is complex and not well understood. Soft, easily hardened materials sink-in whereas harder, work-hardened materials pileup [27]. In general, dislocations will be generated in the material near the tip of the indenter. The propagation of these dislocations along the available slip planes in the material will be governed by the applied load (i.e. resolved shear stress along the slip plane). If resolved shear stress is higher than the critical resolved shear stress (CRSS) required for the propagation of the dislocations, these dislocations could propagate along the slip plane and could move downwards into the material or cross-slip to the surface of the indent generating pileup. In case of heavily work-hardened (low yield stress) RD (due to repetitive rolling during fabrication), RD's capacity for downward dislocation motion into the indent could reach its peak sooner than in TD, thus increasing the propensity for cross-slip on the available slip planes and then generating a higher pileup in RD in comparison to TD.

## 4.2 Pileup profile

The pile-up of material during nanoindentation is highly dependent on its crystallographic texture. Further, the height of the pileup can vary on the same surface plane indicating a strong influence of slip geometry leading to plastic anisotropy as observed along RD and TD in 16 nm Cu/Nb ARB nanolaminate. In the case of Cu/Nb ARB nanolaminate, the crystallographic axes aligned along the normal direction (ND) can range from [4 4 11], [110] to [112] depending on the Cu layer thickness [13]. Similarly, for Nb, the ND can range from [3 3 -8], to [112] depending on the layer thickness. For the 16 nm Cu/Nb ARB sample, 4 axis diffractometer was used to obtain crystallographic axes aligned along the normal direction, rolling direction and

transverse direction (see Figures 1 and 2). For Cu, ND is [1 1 2], RD is [1 -1 0] and TD is [-1 -1 1] and for Nb, ND is [1 1 2], RD is [1 1 1] and TD is [1 1 0]. Typically, in order to document the effect of crystallographic texture on the nature of surface pileup, it is advisable to document activated slip systems with respect to TD and RD [28]. In particular, for FCC Cu, there are 12 slip systems. Dislocation along a slip plane is triggered when the shear stress along that slip plane reaches the critical resolved shear stress. Therefore, CRSS (or Schmid factor) can be calculated for available slip systems along RD and TD to document activated slip systems along RD and TD. Nevertheless, Berkovich indenter (in comparison to conical or spherical indenter) imposes a complex stress field under the indenter which can result in non-uniformly activated slip systems which make it difficult to directly compare Schmid factor calculations to the experimental results such as surface pileups.

Apart from the material plasticity, plasticity at the Cu/Nb interface also affects the pileup. Demkowicz *et al.* [24] had documented interface shear strength along TD is 1.2 GPa whereas it is infinite along RD. The infinite shear strength along RD allows for co-deformation of layers and subsequently high pileup in comparison to TD where the interface has the capacity of slide [8–12, 16].

## 5 Conclusions

The present analysis performed nanoindentation on 16 nm Cu/Nb ARB nanolaminates as a function of the indentation depth. The surface pileup was found to be higher along RD than along TD which is attributed to their crystallographic and interfacial anisotropy. These anisotropy along RD and TD results in higher yield strength (low plasticity) along TD in comparison to RD. Interfacial anisotropy also contributes to interfacial sliding in the case of TD resulting in less co-deformation of layers in comparison to RD. Both these factors contribute to higher pileup along RD in comparison to TD.

## 6 Acknowledgement

We gratefully acknowledge co-funding provided by the National Research Foundation (NRF) of the Singapore's government through the Grant NRF2018-NRF-ANR042 (Street Art Nano) and the ANR (Agence Nationale de la Recherche) of the France's government through the Grant ANR ANR18-CE09-003801 (Street Art Nano). ASB, FEG and CH also gratefully acknowledge funding from BINUS University in the form of PIB (Penelitian Internasional BINUS; BINUS International Collaboration Research) through the Grant PIB006/2021.

## 7 References

1. Zhang GP, Liu Y, Wang W, Tan J (2006) Experimental evidence of plastic deformation instability in nanoscale Au⁄Cu multilayers. Appl Phys Lett 88:13105
2. Li YP, Zhu XF, Tan J, et al (2009) Comparative investigation of strength and plastic instability in Cu/Au and Cu/Cr multilayers by indentation. J Mater Res 24:728–735
3. Li YP, Zhu XF, Zhang GP, et al (2010) Investigation of deformation instability of Au/Cu multilayers by indentation. Philos Mag 90:3049–3067
4. Gerberich WW, Kramer DE, Tymiak NI, et al (1999) Nanoindentation-induced defect–interface interactions: phenomena, methods and limitations. Acta Mater 47:4115–4123
5. Esqué-de los Ojos D, Očenášek J, Alcalá J (2014) Sharp indentation crystal plasticity finite element simulations: Assessment of crystallographic anisotropy effects on the mechanical response of thin fcc single crystalline films. Comput Mater Sci 86:186–192
6. Biener MM, Biener J, Hodge AM, Hamza A V (2007) Dislocation nucleation in bcc Ta single crystals studied by nanoindentation. Phys Rev B 76:165422
7. Morris JR, Bei H, Pharr GM, George EP (2011) Size effects and stochastic behavior of nanoindentation pop in. Phys Rev Lett 106:165502

8. Budiman AS, Sahay R, Ali HPA, et al (2020) Interface-mediated plasticity and fracture in nanoscale Cu/Nb Multilayers as revealed by in situ clamped microbeam bending. Mater Sci Eng A 140705
9. Ali HPA, Radchenko I, Li N, Budiman A (2018) The roles of interfaces and other microstructural features in Cu/Nb nanolayers as revealed by in situ beam bending experiments inside an scanning electron microscope (SEM). Mater Sci Eng A 738:253–263
10. Ali HPA, Radchenko I, Li N, Budiman A (2019) Effect of multilayer interface through in situ fracture of Cu/Nb and Al/Nb metallic multilayers. J Mater Res 34:1564–1573
11. Tian T, Morusupalli R, Shin H, et al (2016) On the mechanical stresses of cu through-silicon via (tsv) samples fabricated by sk hynix vs. sematech–enabling robust and reliable 3-d interconnect/integrated circuit (ic) technology. Procedia Eng 139:101–111
12. Ali HPA, Budiman A (2019) Advances in In situ microfracture experimentation techniques: A case of nanoscale metal–metal multilayered materials. J Mater Res 34:1449–1468
13. Beyerlein IJ, Mara NA, Carpenter JS, et al (2013) Interface-driven microstructure development and ultra high strength of bulk nanostructured Cu-Nb multilayers fabricated by severe plastic deformation. J Mater Res 28:1799–1812
14. Mara NA, Bhattacharyya D, Dickerson P, et al (2008) Deformability of ultrahigh strength 5 nm Cu⁄Nb nanolayered composites. Appl Phys Lett 92:231901
15. Demkowicz MJ, Hoagland RG, Hirth JP (2008) Interface structure and radiation damage resistance in Cu-Nb multilayer nanocomposites. Phys Rev Lett 100:136102
16. Radchenko I, Anwarali HP, Tippabhotla SK, Budiman AS (2018) Effects of interface shear strength during failure of semicoherent metal–metal nanolaminates: An example of accumulative roll-bonded Cu/Nb. Acta Mater 156:125–135

17. Fischer-Cripps AC, Nicholson DW (2004) Nanoindentation. Mechanical engineering series. Appl Mech Rev 57:B12–B12

18. Mitchell TE, Lu YC, Jr AJG, et al (1997) Structure and mechanical properties of copper/niobium multilayers. J Am Ceram Soc 80:1673–1676

19. Beyerlein IJ, Mara NA, Wang J, et al (2012) Structure–property–functionality of bimetal interfaces. Jom 64:1192–1207

20. Zheng S, Beyerlein IJ, Carpenter JS, et al (2013) High-strength and thermally stable bulk nanolayered composites due to twin-induced interfaces. Nat Commun 4:1696

21. Carpenter JS, McCabe RJ, Zheng SJ, et al (2014) Processing parameter influence on texture and microstructural evolution in Cu-Nb multilayer composites fabricated via accumulative roll bonding. Metall Mater Trans A 45:2192–2208

22. Kocks UF, Tomé CN, Wenk H-R (1998) Texture and anisotropy: preferred orientations in polycrystals and their effect on materials properties. Cambridge university press

23. Beyerlein IJ, Mara NA, Wang J, et al (2012) Structure-property-functionality of bimetal interfaces. JOM 64:1192–1207. https://doi.org/10.1007/s11837-012-0431-0

24. Demkowicz MJ, Thilly L (2011) Structure, shear resistance and interaction with point defects of interfaces in Cu–Nb nanocomposites synthesized by severe plastic deformation. Acta Mater 59:7744–7756

25. Oliver WC, Pharr GM (1992) An improved technique for determining hardness and elastic modulus using load and displacement sensing indentation experiments. J Mater Res 7:1564–1583

26. Nizolek T, Beyerlein IJ, Mara NA, et al (2016) Tensile behavior and flow stress anisotropy of accumulative roll bonded Cu-Nb nanolaminates. Appl Phys Lett 108:2–6. https://doi.org/10.1063/1.4941043

27. Cheng Y-T, Cheng C-M (2000) What is indentation hardness? Surf Coatings Technol

133:417–424

28. Casals O, Očenášek J, Alcala J (2007) Crystal plasticity finite element simulations of pyramidal indentation in copper single crystals. Acta Mater 55:55–68